

PACS numbers: 42.30.Va; 42.79.Hp; 42.79.Kr
DOI: 10.1070/QE2000v030n07ABEH001777

Controlled optical structures in a nonlinear system involving the suppression of low spatial frequencies in the feedback loop

I P Nikolaev, A V Larichev, V I Shmal'gauzen

Abstract. A nonlinear optical system with spatially distributed feedback was studied both theoretically and experimentally. The phase-to-intensity transformation in this system was performed by a spatial filter capable of suppressing low spatial frequencies. Hard excitation of stationary spatial structures observed in this system was explained by an analysis of the phase space structure of the amplitude equations. The developed theoretical approach, which uses a step-function approximation of the steady-state solution, allows one to determine the main quantitative characteristics of the generated structures. The basic properties of the response of the system to external perturbations with various symmetries were investigated experimentally. The obtained experimental data qualitatively agree with the results of the theoretical analysis.

1. Introduction

Nonlinear optical systems with spatially distributed feedback are interesting and promising objects of investigation. Possible applications, the most well-known of which is the high-resolution wavefront correction [1, 2], and the opportunity to consider the problem of self-organisation in optics [3, 4] have stimulated the development of experimental investigations [5 – 7] as well as theoretical models and methods for their analysis [8 – 10].

The nonlinear system with optical feedback can be realised with a liquid-crystal (LC) spatial light modulator (SLM) [5, 6]. In an LC SLM, the incident plane light wave is reflected by the internal dielectric mirror, thereby making it transverse the LC layer twice. The reflected wave then goes through the feedback loop and falls upon the photosensitive surface of the LC SLM. The nonlinear phase shift that the initial wave acquires in the LC layer is controlled by the distribution of the radiation intensity in the feedback loop, which also represents the output radiation of the system. The feedback loop produces the intensity distribution, which depends on the phase modulation of the wave reflected by the modulator. In this way, it performs a certain phase-to-intensity transformation.

I P Nikolaev, A V Larichev, V I Shmal'gauzen Physics Department, M V Lomonosov Moscow State University, Vorob'yovy Gory, 119899 Moscow, Russia

Received 26 November 1999
Kvantovaya Elektronika **30** (7) 617 – 622 (2000)
Translated by I V Bargatin; edited by M N Sapozhnikov

For most of the similar nonlinear optical systems investigated up to this moment, soft excitation is typical: The generated structures can develop from initial fluctuations of arbitrarily small amplitude. However, soft excitation is not a universal property of such systems [8, 11, 12]. In contrast, the systems with hard excitation are sensitive to both the amplitude and the spatial structure of external disturbance; therefore, such optical systems may have applications in optical devices for data processing.

In this work, we consider a nonlinear optical system with spatially distributed feedback, which shows hard excitation of optical structures. The system contains an amplitude spatial filter that acts as a phase-to-intensity transformer. This filter consists of a confocal $4f$-system that contains a small opaque disk in its Fourier plane, which masks the zero order of the spatial spectrum of the feedback radiation. This phase visualisation system belongs to the 'dark field' class of devices [13].

2. Analysis of stability of the steady-state solutions

The dynamics of the nonlinear phase modulation $u(\mathbf{r}, t)$ that is acquired by the light wave reflected from the LC SLM can be described by the relaxational Debye-type equation [1]

$$\tau \frac{\partial u(\mathbf{r}, t)}{\partial t} + u(\mathbf{r}, t) = l_{\mathrm{d}}^2 \Delta_{\perp} u(\mathbf{r}, t) - \chi I_{\mathrm{fb}}(\mathbf{r}, t). \quad (1)$$

Here, τ is the LC molecule relaxation time; l_{d} is the diffusion length that characterises the finite spatial resolution of the LC SLM [14]; $\chi > 0$ is the sensitivity of the LC SLM; $I_{\mathrm{fb}}(\mathbf{r}, t)$ is the intensity of the feedback field. The minus sign in front of the last term of the equation corresponds to the decreasing dependence of the phase shift acquired in the LC layer of the modulator on the intensity of the light incident on the photoconductor [15, 16].

The intensity of the feedback field can be written in the form

$$I_{\mathrm{fb}}(\mathbf{r}, t) = I_0 \eta g(\mathbf{r}, t), \quad (2)$$

where I_0 is the intensity of the incident wave; η is the overall transmission coefficient of the passive optical elements of the feedback loop; g is the dimensionless (normalised to I_0) feedback signal. For the system considered, we will define the feedback factor as

$$K \equiv \eta \chi I_0. \quad (3)$$

The relationship between the functions g and u is determined by the chosen method of the spatial filtering of the field

having the complex amplitude e^{iu}, which takes place in the feedback loop. Suppose that our filter suppresses only the zero Fourier component of this complex amplitude distribution, that is, subtracts from it its spatial average $\langle e^{iu} \rangle$. Equation (1) can therefore be rewritten in the form

$$\tau \frac{\partial u(x,t)}{\partial t} + u(x,t) = l_d^2 \frac{\partial^2 u(x,t)}{\partial x^2} - Kg(x,t)\,,$$
$$g(x,t) = \left| e^{iu(x,t)} - \langle e^{iu(x,t)} \rangle \right|^2. \tag{4}$$

Here, we restrict our consideration to the one-dimensional case, $\mathbf{r} = \{x\}$.

It is easy to verify that if the function $u(x,t)$ is a sinusoidal phase grating with spatial frequency v_0, the intensity of the feedback field will be modulated at the double frequency $2v_0$. Therefore, a sinusoidal grating cannot be generated by the con-sidered system since it is not a 'self-sustaining pattern', as is, for example, a roll in the diffractional scheme [9].

Assume now that the phase modulation in the nonlinear medium layer consists of two spectral components with multiple frequencies v_0 and $2v_0$. Then, we have for the two small modulation amplitudes a_1 and a_2

$$e^{iu} = \exp\{i[a_1(t)\cos v_0 x + a_2(t)\cos 2v_0 x]\}$$
$$\approx 1 + i[a_1(t)\cos v_0 x + a_2(t)\cos 2v_0 x]. \tag{5}$$

The complex amplitude $A_{out}(x,t)$ of the filtered field is

$$A_{out}(x,t) \approx i[a_1(t)\cos v_0 x + a_2(t)\cos 2v_0 x], \tag{6}$$

and, neglecting the spectral components of frequencies higher than $2v_0$, the intensity of the filtered field is given by

$$g(x,t) = |A_{out}(x,t)|^2$$
$$= \frac{a_1^2(t) + a_2^2(t)}{2} + a_1 a_2 \cos v_0 x + \frac{a_1^2}{2}\cos 2v_0 x + \ldots \tag{7}$$

One can see that the distribution of the feedback field intensity contains the terms of both the frequencies $2v_0$ and v_0. It is therefore reasonable to assume that these two harmonics will develop cooperatively when the feedback loop is closed.

By inserting into Eq. (4) the feedback field intensity from expression (7) as well as the phase modulation $u(x,t)$ in the form of a superposition of two harmonics with the time-dependent amplitudes a_1 and a_2, we obtain the system of amplitude equations

$$\tau \dot{a}_1 = -a_1 - K a_1 a_2,$$
$$\tau \dot{a}_2 = -a_2 - K a_1^2/2. \tag{8}$$

Here, we use the weak diffusion approximation; we assume condition $v_0 l_d \ll 1$ is fulfilled. The system of ordinary differential equations (8) has three singular points: the stable node $0,0$ and two saddle points, $\sqrt{2}/K, -1/K$ and $-\sqrt{2}/K, -1/K$. Fig. 1 shows their arrangement in the phase space a_1, a_2. Such configuration of singular points corresponds to the hard excitation mode. This means that if the initial amplitudes are small with respect to $O(1/K)$, the system 'slides back' to the trivial solution. Conversely, if the initial amplitudes lie in the other direction from the saddle surface, they will grow until the nonlinear restrictive mechanism, which is not accounted for in the reduced system (8), comes into play.

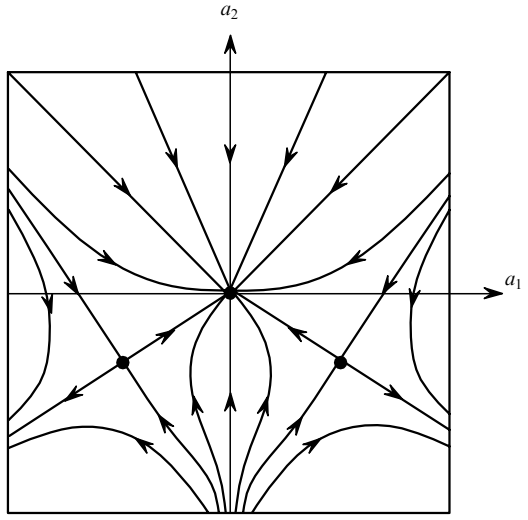

Figure 1. Qualitative picture of phase trajectories and singular points of the reduced system (8).

The above analysis, however, allows us to explain the hard excitation only qualitatively and does not provide any quantitative details. To verify the predictions of the above approximate analysis, we investigated this problem numerically. Fig. 2 shows the steady-state solution of Eq. (4). The boundary conditions were chosen to be periodic in accordance with the plane wave approximation. One can see that the shape of the phase grating is almost rectangular. This means that its spectrum contains many harmonics, and, therefore, the reduced system (8) is not adequate for obtaining quantitative results.

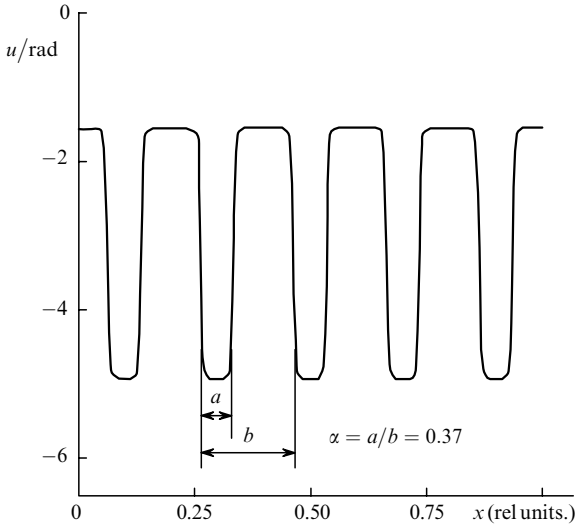

Figure 2. Steady-state solution of equation (4) for $K = 3$, $v_0 l_d = 0.1$ and the initial phase modulation $u_0(x) = \cos v_0 x$, $v_0 = 10\pi$.

The period of the generated grating is defined exclusively by the initial conditions because the suppression of the zero Fourier component does not lead to any frequency selectivity. The diffusion only contributes to smoothing of the steady-state solution. Thus, the considered system can be characterised by hard excitation and the sensitivity of the steady-state solution to the initial conditions.

3. The step-function approximation of the steady-state solution

One can see from Fig. 2 that the generated structure can be accurately described as a periodic sequence of zones where the phase $u(x)$ assumes one of the two 'quantised' values. In the distribution of the feedback field intensity $g(x)$, this corresponds to a periodical structure of dark (Σ_1) and bright (Σ_2) zones. If we neglect the existence of the transition zones, the steady-state solution of Eq. (4) can be rewritten in the form

$$u(x) = \begin{cases} -u_1, x \in \Sigma_1 \\ -u_2, x \in \Sigma_2. \end{cases} \tag{9}$$

Then, the complex amplitude of the field at the filter input is

$$A_{\text{in}}(x) = \begin{cases} \exp(-\mathrm{i}u_1), \ x \in \Sigma_1 \\ \exp(-\mathrm{i}u_2), \ x \in \Sigma_2. \end{cases} \tag{10}$$

The spatial filtering results in the suppression of the zero Fourier component, whose amplitude S_0 equals the average value of the function $A_{\text{in}}(x)$,

$$S_0 = \alpha \exp(-\mathrm{i}u_2) + (1-\alpha)\exp(-\mathrm{i}u_1), \tag{11}$$

where α is the relative area of the bright zones. From Eqs (10) and (11), we obtain the following expression for the complex field amplitude at the filter output

$$A_{\text{out}}(x) = A_{\text{in}}(x) - S_0 = \begin{cases} \alpha\left(\mathrm{e}^{-\mathrm{i}u_1} - \mathrm{e}^{-\mathrm{i}u_2}\right), \ x \in \Sigma_1, \\ (1-\alpha)\left(\mathrm{e}^{-\mathrm{i}u_2} - \mathrm{e}^{-\mathrm{i}u_1}\right), \ x \in \Sigma_2. \end{cases} \tag{12}$$

Calculating the square modulus of these equations, we derive the intensity distribution of the feedback field

$$g(x) = \begin{cases} 2a^2[1-\cos(u_2-u_1)] \equiv I_1, \ x \in \Sigma_1, \\ 2(1-a)^2[1-\cos(u_2-u_1)] \equiv I_2, \ x \in \Sigma_2. \end{cases} \tag{13}$$

By inserting expressions (9) and (13) into Eq. (4) and neglecting the diffusion term*, we obtain the following system of nonlinear algebraic equations for the upper and lower 'quantised' values of the steady-state phase

$$\begin{aligned} u_1 &= 2K\alpha^2(1-\cos\Delta u), \\ u_1 + \Delta u &= 2K(1-\alpha)^2(1-\cos\Delta u), \end{aligned} \tag{14}$$

where $\Delta u \equiv u_2 - u_1$. Note that the above calculations are also valid for the two-dimensional case; therefore, we can assume that $u = u(\mathbf{r})$.

The system (14) contains three unknown variables: u_1, Δu, and α and, therefore, we have to involve some additional arguments to solve it. For example, we can consider the energy aspect of the problem. For sufficiently small initial phase modulations, the system returns to the zero equilibrium position (see Fig. 1). This means that the total energy of the light wave is concentrated in the zero spectral order, which is masked by the filter. The feedback loop is fully darkened in this case.

On the other hand, if the initial phase modulation is sufficient to excite a nontrivial solution, the amplitudes of the spatially nonuniform components begin to grow. This leads to a corresponding redistribution of the energy from the zero order to the higher orders. Let us assume that this process results in the establishment of the steady-state solution in which the filter absorbs the minimal possible power. The integral power P_{fb} of the feedback signal (which is normalised as to satisfy $P_{\text{fb}} = 1$ in the absence of the filter) can be easily expressed in terms of Δu by reshaping Eqs (11) and (14),

$$P_{\text{fb}} = 1 - S_0 S_0^* = \frac{(1-\cos\Delta u)^2 - (\Delta u/2K)^2}{2(1-\cos\Delta u)}. \tag{15}$$

In this way, we can formulate the following procedure for calculation of all unknown variables. For a given K, we find the maximum of the function $P_{\text{fb}}(\Delta u)$ and the corresponding argument Δu. Then, we express the quantities in which we are interested through the following formulas, which are direct consequences of Eqs (13) and (14):

$$\alpha = \alpha(K, \Delta u) = 0.5 - \frac{\Delta u}{4K(1-\cos\Delta u)}, \tag{16}$$

$$u_1 = u_1(K, \Delta u) = \frac{[2K(1-\cos\Delta u) - \Delta u]^2}{8K(1-\cos\Delta u)}, \tag{17}$$

$$u_2 = u_2(K, \Delta u) = \frac{[2K(1-\cos\Delta u) + \Delta u]^2}{8K(1-\cos\Delta u)}, \tag{18}$$

$$I_1 = I_1(K, \Delta u) = \frac{[2(1-\cos\Delta u) - \Delta u/K]^2}{8(1-\cos\Delta u)}, \tag{19}$$

$$I_2 = I_2(K, \Delta u) = \frac{[2(1-\cos\Delta u) + \Delta u/K]^2}{8(1-\cos\Delta u)}. \tag{20}$$

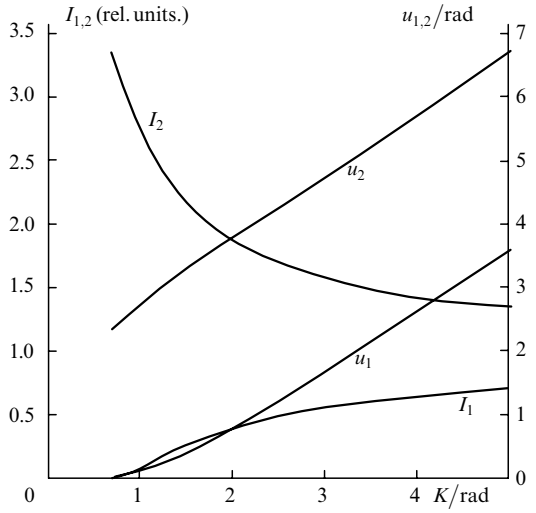

Figure 3. Steady-state phase shifts and the feedback field intensities as functions of the feedback factor.

* The diffusion term is important only in the transition zone, which we neglect in this approach.

Relationships (16)–(20) are illustrated by the curves shown in Fig. 3 and Fig. 4. One can see from these figures that the critical feedback factor amounts to $K_c \approx 0.7$, and that for $K < K_c$ no solutions of the considered type can be generated. For large values of K, we have the following asymptotic behaviour of the parameters of the steady-state solution: $\Delta u \to \pi$, $P_{fb} \to 1$, $\alpha \to 0.5$, $u_1 \to K - \pi/2$, $u_2 \to K + \pi/2$, $I_1 \to 1 - \pi/2K$, $I_2 \to 1 + \pi/2K$.

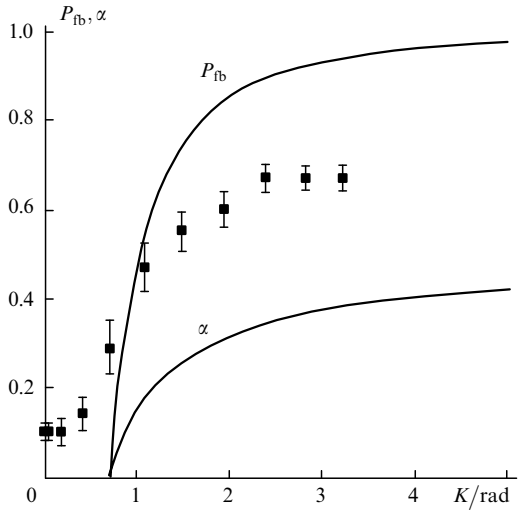

Figure 4. Steady-state total power of the feedback field and the relative area of bright zones as functions of the feedback factor. Squares represent the experimentally measured power.

Note that the results of the step-function approximation were fully confirmed by the numerical solution of Eq. (4) for the case of weak diffusion ($l_d v_0 \ll 1$). Thus, we corroborate the intuitive assumption that the closed system tends toward the state of the maximal possible rate of energy transfer from the zero order to higher orders.

4. Experimental setup

The experimental setup is shown the Fig. 5. We used a 50-mW helium-neon laser (*1*) ($\lambda = 632.8$ nm) as the radiation source. The laser beam was widened to a diameter of 4 cm by the confocal system of the microscope objective (*2*) and the objective (*4*). After reflection from the internal mirror of the LC SLM (*5*), the beam was limited to a diameter of 1.2 cm (the operating aperture of the modulator) and directed into the feedback loop.

The feedback loop contains two identical objectives (*3*) and (*4*) with the focal distance $f = 70$ cm and the spatial filter (*6*) that is centred on the optical axis. The filter consists of a thin glass substrate, which has an opaque circle on it with a diameter of 350 μm, and an iris diaphragm, which is centred on the circle to filter the high-frequency noise. The lower bound of the spatial frequencies transmitted by this filter equals approximately 25 cm^{-1}, which corresponds to a structure that contains 4 periods on a 1-cm length; the upper bound can be varied by adjusting the diaphragm diameter. The image that is formed at the output plane of the spatial filter is transferred by the optical fibre bundle (*9*) onto the photoconductive layer of the LC SLM. Rotating the polariser (*8*) varies the feedback factor.

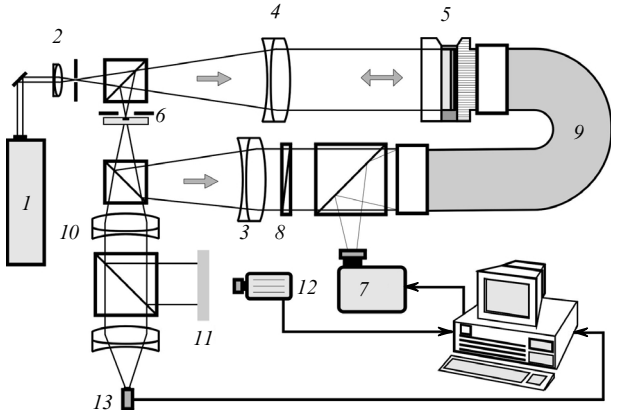

Figure 5. Experimental setup: (*1*) He-Ne laser; (*2*) microscope objective; (*3*) and (*4*) 4*f*-system objectives; (*5*) LCLV; (*6*) spatial filter; (*7*) LC projector; (*8*) polariser; (*9*) optical fibre cable; (*10*) objective of the detection system; (*11*) ground glass screen; (*12*) CCD camera; (*13*) photodetector.

The detection system consists of a CCD camera (*12*), which is connected to a PC via a frame grabber, and a photodetector (*13*). The camera detects the intensity distribution of the feedback loop field I_{fb}, which is formed by the objective (*10*) on the ground glass screen (*11*). The photodetector measures the total power of the feedback signal.

In the theoretical part of this paper, we assumed that the external disturbance of the system produces some controlled phase distribution, which plays the role of the initial conditions at the moment of the feedback loop closing. However, it is hard to realise this situation experimentally because inhomogeneities that are present in the LC SLM will destabilise and destroy the structure created (because the autonomous system does not possess a definite attractor). It is therefore reasonable to turn our attention to the dynamics of the non-autonomous system. The non-autonomous system is realised whenever some permanent spatially-nonuniform external disturbance is maintained after the closing of feedback loop. The external disturbance was produced by an LC video projector (*7*), which projected a computer-generated image onto the entry surface of the optical fibre bundle. In this way, we could easily control the amplitude and the shape of the external disturbance.

Consider now how the behaviour of the closed system changes when an external optical field acts permanently on it. This external field produces additional stationary phase modulation of the wave reflected from the LC SLM. An analysis similar to that of Section 2 demonstrates that the qualitative behaviour of the closed system remains the same: In order to initialise self-excitation, the amplitude of the external additional phase modulation produced by the external field must exceed a critical amplitude, which depends on the feedback factor. However, this critical amplitude is much smaller than that of the autonomous system. This can be explained by the fact that the feedback loop now receives a permanent inflow of energy rather than an initial boost, as in the autonomous system.

The method of amplitude equations, in principle, allows one to determine the threshold amplitudes for both the autonomous and the non-autonomous problems. However, in order to attain the necessary accuracy of the results, one has to include a large number of harmonics into consideration, which leads to rather bulky calculations. It is therefore

more reasonable to determine the threshold amplitude dependences by means of numerical simulation.

The corresponding curves are shown in Fig. 6. The dashed curve shows the threshold amplitude of a sinusoidal phase grating, which represents the initial phase modulation in the LC SLM, as a function of the feedback factor. The solid curve corresponds to a permanently maintained grating of the same form. One can see that the self-excitation thresholds differ by a factor of 4 to 5 in these two situations.

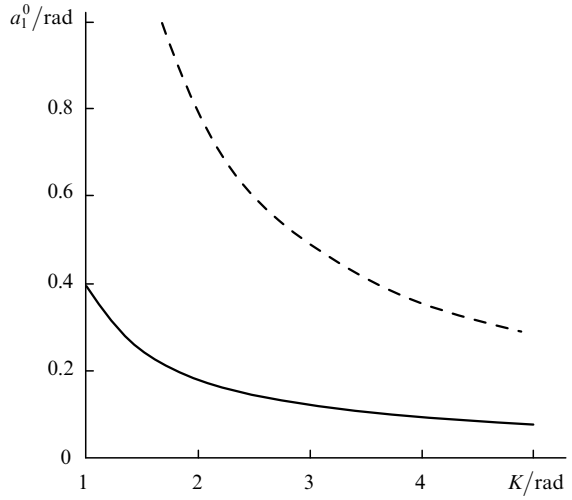

Figure 6. Numerically calculated dependence of the excitation threshold on the feedback factor for $v_0 l_d = 0.1$. The dashed curve represents an autonomous system with the initial phase modulation of the form $u_0(x) = a_1^0 \cos v_0 x$. The solid curve represents a non-autonomous system with an additional stationary phase modulation of the same form.

For sufficiently large K, the threshold amplitude of the external perturbation (in the non-autonomous configuration) is negligible with respect to the steady-state phase calculated in Section 3. Therefore, the dependences obtained by means of the step-function approximation are also relevant for the non-autonomous system, provided that the amplitude of the external perturbation is not much larger than the threshold amplitude.

5. The response of the closed system to various external perturbations

To investigate the dynamics of the non-autonomous system, we chose model objects of various symmetries, which were projected onto the entry surface of the optical fibre bundle by the video projector. This created a stationary 'seed' distribution of the phase of the wave reflected from the LC SLM. Two of these model objects are shown in Fig. 7: a hexagon (Fig. 7 a) and a set of equidistant concentric circles (Fig. 7 b). The photographs of the feedback loop field distribution, also shown in Fig. 7, are arranged as follows. The second row corresponds to the opened feedback loop, the third and the fourth rows, to the closed feedback loop. The two columns, in which the photographs of the responses are arranged in, refer to the respective objects.

Duplication of the spatial frequencies of harmonic components of the phase distribution is a characteristic feature of the phase-to-intensity transformation performed by our spatial filter. This effect is clearly demonstrated in Fig. 7 d, which shows that the number of circles increased by a factor of two with respect to Fig. 7 b. For the hexagon, this effect results merely in the appearance of the halos around the spots of the honeycomb-like structure.

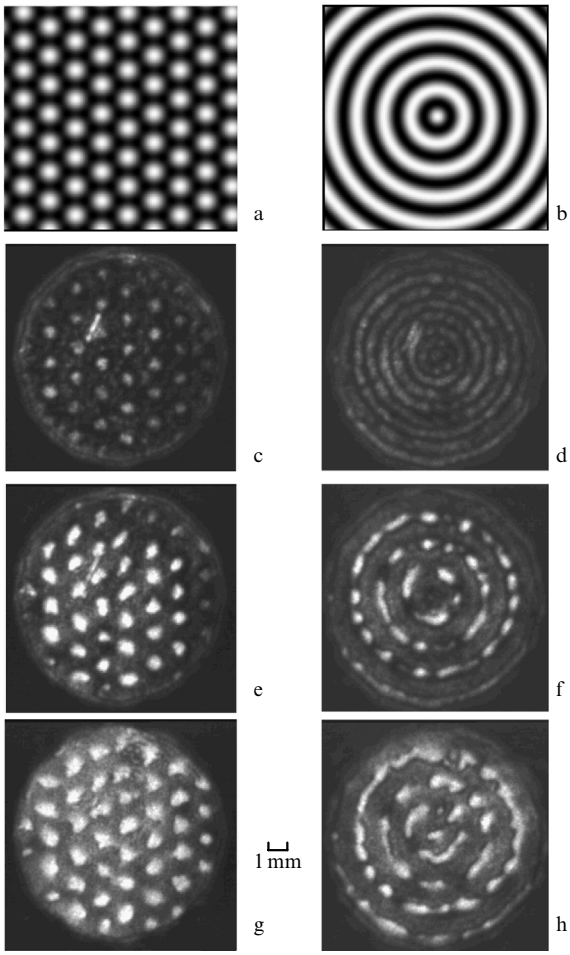

Figure 7. Images projected on the photoconductor of the LCLV (a, b) and the photographs of the corresponding distributions of the feedback field for the following values of the feedback factor: $K = 0$ (c, d), $K = 1.1$ (e, f), and $K = 3.2$ (g, h).

When the feedback loop is closed, the characteristics of the output image strongly depend on the feedback factor. For $K = 0.7$ (not shown in Fig. 7), the fraction of energy that is redistributed from the zero spectral order into higher orders is still too small. However, the incipient structure formation is already discernible: The fundamental spatial frequency begins to dominate the double frequency. For $K = 1.1$ (Figs 7 e and 7 f), the total power of the feedback signal is substantially larger, and the image contrast is quite high. For large values of K (Figs 7 g and 7 h), the contrast decreases and the area of the bright zones increases. These properties of the generated structures are in qualitative agreement with the theoretical dependences shown in Figs 3 and 4.

However, we observed some effects that were not accounted for by theory in the experiments. In particular, for large values of K, we observed distortion of the regular structures that was imposed by the projected images. The effect is most noticeable for 'striped' structures like the circles, which disintegrate into separate spots. Conversely, for the structures that are spot-like from the beginning, we

only observed a certain drift of the spots (due to diffusion of charges in the photoconductor layer of the LC SLM) accompanied by distortion of their shape. These effects may be related to the inevitable internal inhomogeneity of all LC SLMs (of the affordable price range). Fig. 6 shows that, for large values of K, the threshold of hard excitation is very small; therefore, even minor changes in the modulator parameters may result in the appearance of new spectral components.

The normalised total power P_{fb} of the output signal (15) is the most conveniently measured quantitative characteristic of the generated structures. The experimental values of P_{fb} averaged over all the model objects are shown by squares in Fig. 4. Note that the photodetector (*13*) detects the power of the beam before it passes through the polariser (*8*) that controls K. In this way, parametric control of the power of the output signal is realised.

If the projector is turned off, the output field remains dark up to values of $K \approx 2$. A further increase in K results in self-excitation of irregular structures that are triggered by internal inhomogeneities of the modulator and other noise. In accordance with the dependence shown in Fig. 6, the self-excitation threshold can be crossed for $K = 2$ if the root-mean-square deviation of the wave front at the nonlinear element output amounts to $\sim 0.03\lambda$. This demonstrates predictability of such effects in the systems based on LC SLMs.

6. Conclusions

Thus, we have managed to explain theoretically the hard excitation of spatial structures in the nonlinear optical system involving the suppression of low spatial frequencies in the feedback loop. The analytical dependences of the main characteristics of these structures upon the control parameters have been derived. The experimental results qualitatively agree with the predictions of the theoretical model.

The discrepancy observed in Fig. 4 can be explained by the following major causes. For sufficiently small values of K, this discrepancy is evidently caused by the action of the stationary phase modulation created by the projected image. This modulation results in transfer of a fraction of the energy of the wave reflected from the LC SLM, into corresponding spectral orders. For large values of K, this discrepancy is probably caused by saturation of the modulator. For the sample used, the maximum light-induced phase shift amounts to $\sim 2\pi$; in addition, a part of the dynamic range (no less than two radians) is lost due to the influence of the projected image.

The LC SLM is therefore not capable of providing the required stationary phase shifts (see Fig. 3). Nevertheless, the theoretical and experimental threshold values of K are in good agreement, even though the experimental threshold was determined less accurately due to nonuniformity of both the LC SLM characteristics and the incident beam intensity. We can thus conclude that, for quantitative description of the experimental data by means of the theoretical approach considered, the LC SLM must possess a high spatial uniformity and a sufficient dynamical range.

Acknowledgements. This work was supported by the Russian Foundation for Basic Research (Grant No. 98-02-17125).

References

1. Vorontsov M A, Kirakosyan M E, Larichev A V *Kvantovaya Elektron. (Moscow)* **18** 117 (1991) [*Sov. J. Quantum Electron.* **21** 105 (1991)]
2. Pepper D M, Gaeta C J, Mitchell P V, in *Spatial Light Modulator Technology: Materials, Devices and Applications* (New York: Marcel Dekker Inc., 1995, p. 585)
3. Cross M C, Hochenberg M C *Rev. Mod. Phys.* **65** 851 (1993)
4. Arecchi F T *Physica D* **86** 297 (1995)
5. Sengupta U K, Gerlach U H, Collins S A *Opt. Lett.* **3** 199 (1978)
6. Akhmanov S A, Vorontsov M A, Ivanov V Yu *Pis'ma Zh. Eksp. Teor. Fiz.* **47** 611 (1988) [*JETP Lett.* **47** 707 (1988)]
7. Ramazza P, Residori S, Pampaloni E, Larichev A V *Phys. Rev. A* **53** 400 (1996)
8. Rozanov N N, Khodova G V *J. Opt. Soc. Am. B* **7** 1057 (1990)
9. Vorontsov M A Firth W *J Phys. Rev. A* **49** 2891 (1994)
10. Balkareĭ Yu I, Evtikhov M G, Elinson M I, Kogan A S *Kvantovaya Electron. (Moscow)* **24** 625 (1997) [*Quantum Electron.* **27** 608 (1997)]
11. Rakhmanov A N *Opt. Spektrosk.* **74** 1184 (1993) [*Opt. Spectrosc.* **74** 701 (1993)]
12. Rakhmanov A N, Shmalhauzen V I *Proc. SPIE Int. Soc. Opt. Eng.* **2108** 428 (1993)
13. Vasil'ev L A *Tenevye Metody (Shadow Methods)* (Moscow: Nauka, 1968)
14. Wang L, Moddel G *Opt. Lett.* **19** 2033 (1994)
15. Dumarevskiĭ Yu D, Kovnotyuk N F, Savin A I *Preobrazovanie izobrazhenii v strulturakh poluprovodnik-dielektrik (Transformation of Images in Semiconductor-Dielectric Structures)* (Moscow: Nauka, 1987)
16. Vasil'ev A A, Kasasent D, Kompanets I N, Parfenov A A *Prostranstvennye modulyatory sveta (Spatial Modulators of Light)* (Moscow: Radio i Svyaz', 1987)